RC23248 (W0406-088) June 16, 2004
Electrical Engineering

IBM Research Report

Quantum-Based Simulation Analysis of Scaling in Ultra-Thin Body Device Structures

Arvind Kumar, Jakub Kedzierski, Steven E. Laux
IBM Research Division
Thomas J. Watson Research Center
P.O. Box 218
Yorktown Heights, NY 10598

Research Division
Almaden - Austin - Beijing - Haifa - India - T. J. Watson - Tokyo - Zurich

Quantum-Based Simulation Analysis of Scaling in Ultra-Thin Body Device Structures

Arvind Kumar, Jakub Kedzierski, and Steven E. Laux

Abstract

We present self-consistent solutions of ultra-thin body device structures to understand the influence of quantum-mechanical confinement on the predictions of classical scaling theory. We show that two-dimensional electrostatics considerations play a more dominant role than quantum-mechanical effects in the subthreshold behavior of ultra-thin fully-depleted silicon-on-insulator structures. We also show how modifications to the doping profile can be used to alleviate two-dimensional short-channel effects.

I. Introduction

Fully depleted silicon-on-insulator (FDSOI) CMOS is currently considered a promising vehicle for continued MOSFET scaling into the nanometer regime due to its inherently low junction capacitance and its potential for nearly ideal subthreshold swing (SS). Although quantum-mechanical effects are expected to play a central role in SOI structures as dimensions are shrunk, device designers frequently utilize scaling theories based on classical electrostatics arguments to estimate short-channel effects. In the simplest approximation, the electric field at the back interface with the buried oxide (BOX) is assumed to have no normal component [1]. This approach has some validity when the channel doping is sufficiently high that subthreshold conduction occurs primarily at the front interface with the gate oxide. The case of an undoped body – increasingly of interest due to mobility and dopant fluctuation considerations – requires a two-dimensional analysis due to fringing fields in the buried oxide [2], [3], although in the long-channel limit one can utilize the scaling length of a double-gate structure with twice the body thickness [4]. The aim of this work is to understand the deviations of classical scaling theory through fully quantum-mechananical simulations [5], [6], [7] which account for both two-dimensional and quantum confinement effects. In addition, quantum-mechanical simulations are used to illustrate improvements in two-dimensional effects possible through changes in the source/drain doping profiles.

The authors are with the IBM Semiconductor Research and Development Center (SRDC), T. J. Watson Research Center, P.O. Box 218, Yorktown Heights, NY 10598 USA (email: arvkumar@us.ibm.com).

II. ELECTROSTATICS VS. QUANTUM CONFINEMENT

Figure 1 shows the basic geometry of the FDSOI structures studied in this work. In this section, we consider a device with an undoped body, gate length L =15 nm and physical oxide thickness t_{ox} =0.5 nm, and vary the body thickness d. Gate leakage is neglected, and we expect that realization of such a thin oxide will require introduction of a high dielectric constant insulator. For a fully quantum-mechanical two-dimensional solution, we utilize the numerical solver QDAME [6], [7] which accounts for confinement and subband effects through a wave description of current-carrying electrons. We compare the QDAME results to those obtained from the semi-classical drift-diffusion simulator FIELDAY [8], intentionally not invoking its capability to include quantum-mechanical corrections [9]. Throughout this work, the SS is computed at low drain voltage and taken at the same value of drain current for different devices to allow for threshold voltage differences. Figure 2(a) compares FIELDAY and QDAME calculations of the SS as a function of body thickness d. The main quantum-mechanical correction is a modest lowering of the SS arising from the repulsion of the electronic wavefunction from the back interface by approximately 1.5 nm, which improves the gate control on the channel charge. Note that the overall increase in gate capacitance as the body is made thinner overshadows the improvement due to quantum effects, so that the quantum correction to the SS *diminishes* as the body becomes thinner.

In order to compare quantum-mechanical and two-dimensional electrostatics corrections to conventional scaling theory, we also plot in Fig. 2(a) the SS, computed semi-classically using FIELDAY, of a symmetric double-gate device of thickness $2d$. Elimination of the fringing electric fields from the source and drain regions through the BOX results in a lower SS than for the FDSOI device; the computed double-gate SS is in excellent agreement with the expected values from one-dimensional scaling theory [4]. We can thus calculate two corrections – $\Delta\mathrm{SS}_{\mathrm{QM}}$ arising from quantum-mechanical effects and $\Delta\mathrm{SS}_{\mathrm{el}}$ arising from two-dimensional electrostatics effects – to the semi-classically computed SS: $\Delta\mathrm{SS}_{\mathrm{QM}}$ is defined as the difference between the FIELDAY- and QDAME-computed SS values for the FDSOI structure, and $\Delta\mathrm{SS}_{\mathrm{el}}$ is defined as the difference between the FIELDAY-computed SS values for the FDSOI and double-gate structures. Figure 2(b) shows $\Delta\mathrm{SS}_{\mathrm{QM}}$ and $\Delta\mathrm{SS}_{\mathrm{el}}$ as a function of the ratio L/λ_u, where $\lambda_u = (\lambda_d^2 + d^2/2)^{1/2}$ is the one-dimensional scaling length for undoped body, with $\lambda_d^2 = dt_{ox}(\epsilon_{Si}/\epsilon_{ox})$, ϵ_{Si} and ϵ_{ox} being the body and insulator dielectric permittivities, respectively [1]. The correction due to two-dimensional electrostatics, $\Delta\mathrm{SS}_{\mathrm{el}}$, is seen to be significantly larger than the quantum one, $\Delta\mathrm{SS}_{\mathrm{QM}}$, which vanishes in the long-channel, or thin-body, limit.

Analysis of the curves in Fig. 2(a) finds, to an excellent approximation, a quadratic dependence of SS on body thickness. The curvature of the quantum-mechanically computed SS is slightly less than that of the semi-classically computed one, reflecting the improved control of the gate on channel charge; the double-gate device, with no fringing fields, has the lowest curvature.

III. BODY DOPING

Doping the body of an FDSOI device improves the electrostatic control of the gate on the channel by shifting the subthreshold leakage path from the back interface to the front interface [3]. In this section, we calculate the SS as a function of uniform body doping to generate a "doping transfer curve" similar to that in Ref. [3]. We simulate two FDSOI structures of different dimensions such that the smaller one has $L = 15$ nm, $t_{ox} = 0.5$ nm, and $d = 5$ nm, and the larger one has $L = 30$ nm, $t_{ox} = 1.0$ nm, and $d = 10$ nm. These dimensions have been chosen so that the two structures have gate-to-scaling length ratios $L/\lambda_u = 3.35$ and $L/\lambda_d = 5.48$ that are equivalent (even when λ_u is corrected for two-dimensional effects in the gate oxide [10]); they are also expected to have the same asymptotic values of SS of 120 mV/dec and 74 mV/dec in the undoped and doped limits, respectively [3].

Doping transfer curves for the two devices are shown in Fig. 3(a-b). Both show a general character of a rapid transition from higher to lower SS as the body doping is increased. In the undoped limit, the larger device has a FIELDAY-computed SS close to the value 120 mV/dec expected from Ref. [3]. Although the same limiting value is expected for the smaller device, the simulated value is somewhat less than this because of the finite width of the electron distribution at the back interface which becomes more important as the body becomes thinner. The QDAME-computed SS values are somewhat lower than the FIELDAY-computed ones due to wavefunction repulsion from the back interface. In the doped limit, one expects the opposite to be true: wavefunction repulsion from the front interface increases the quantum-mechanically computed SS above the semi-classical value obtained from FIELDAY. Results on the smaller device show this to be the case as the doped limit is approached, although the ultrathin body makes this limit effectively unattainable. In the larger device, the transition value of the doping is lower, but the body becomes partially depleted as the doping is increased. Since the threshold voltage is higher when computed quantum-mechanically, the body is less partially depleted in the QDAME simulations for the same current, leading to an improvement in the SS which offsets the degradation due to quantum effects. Thus, in summary, the general effect of the quantum-mechanical correction on the doping transfer curve is the narrowing of the SS window from its classical undoped and doped limits.

IV. ELECTROSTATICS IMPROVEMENT THROUGH DOPING PROFILE

Most analytical modeling of ultrathin body structures is done under the assumption of uniform block doping in the source and drain regions. A simple charge-sharing picture of the FDSOI device [2] shows that the body charge is increasingly controlled by the source and drain as the back interface is approached, leading to loss of gate control and worsening two-dimensional effects. This picture suggests that the two-dimensional effects can be alleviated by tapering the source and drain doping as the back interface is approached, as illustrated by the tapered profile indicated by the dashed line in Fig. 1. Figure 4(a-b) contrasts the potential contours obtained from block doping to those from a tapered doping. Here the tapered doping (uniform in the source and drain) has an abrupt junction lying along one quarter of an ellipse of horizontal axis r and

vertical axis d, as illustrated in the inset of Fig. 5(a), so that increasing r with fixed d increases the degree of tapering. The simulated device has the dimensions of the smaller device described in the previous section, and the metallurgical junction separation at the front interface is 15 nm as before, increasing to 35 nm at the back interface. The equipotential lines are seen to be far more vertical for the tapered doping, so that the electric field is more horizontal at the back interface and two-dimensional effects are reduced. Reduction of two-dimensional effects results in both raising and widening the potential barrier at the leakage path, as shown in Fig. 5(a) by horizontal cuts of the conduction band edge vs. position taken 1.5 nm above the back interface. Figure 5(b) shows the improvement in SS as the degree of tapering is increased by increasing r. It is important to note that this improvement in subthreshold behavior comes at essentially no penalty to drive current, since the conduction path has shifted to the front surface in strong inversion. The inset of Fig. 5(b) illustrates this point by comparing turn-on characteristics for the block vs. tapered case.

V. Discussion and Conclusion

Ultra-thin body structures are among leading candidates for sub-30 nm technologies, but the tradeoff of better electrostatic control at the cost of greater process complexity has not yet led to a clear choice between single-gate FDSOI and double-gate structures. A second issue in sub-30 nm design is whether to use channel doping to control short-channel effects. At these dimensions, channel doping exceeding 10^{19} cm^{-3} is likely to be required, raising concern about Coulomb scattering as well as statistical dopant fluctuations.

To put our findings into perspective, we compare in Fig. 6 the SS for undoped FDSOI, FDSOI with channel doping 2×10^{19} cm^{-3}, and undoped double-gate structure, as a function of body thickness d (the double-gate structure has thickness $2d$). All structures have $L = 15$ nm and $t_{ox} = 0.5$ nm as in Fig. 3(a). The simulations were carried out using QDAME, although a comparison with Fig. 1(a) finds virtually no difference between semi-classically and quantum-mechanically computed SS for the double-gate structures because the leakage path lies in the center for either case. For $d < 3$ nm, the quantum-mechanical repulsion of the wavefunction peak from the back interface moves it to nearly the center of the body independent of whether the body is doped, so that there is little difference between the doped and undoped SS for $d < 3$ nm. As the body thickness is increased, the doped FDSOI maintains its leakage path close to the front interface while in the undoped FDSOI the gate progressively loses control of the leakage path near the back interface, resulting in degraded SS. The undoped double-gate structure of thickness $2d$ is always superior to the undoped FDSOI of thickness d, but its relative advantage diminishes with increasing body thickness. The dashed line in Fig. 6 shows the ratio by which the thickness of the undoped FDSOI must be multiplied to achieve the same SS in a double-gate structure. In the absence of two-dimensional electrostatics and quantum-mechanical corrections, this ratio is exactly two. For very thin body $d < 3$ nm, one might expect the ratio to be less than two because the quantum-mechanical repulsion of the wavefunction shifts the leakage path from the back interface to nearly the middle of the body. However, in accordance with our findings, the ratio is significantly larger than two because this quantum-mechanical benefit is overshadowed by two-dimensional electrostatics. A ratio of two is obtained asymptotically in the limit of thick body.

In conclusion, we have shown through numerical simulations that two-dimensional electrostatics considerations are at least as important as quantum-mechanical ones in understanding the subthreshold scaling behavior of ultra-thin body devices. The subthreshold behavior of UTSOI structures can be improved most strongly through channel doping, but modest improvement is possible through modification of the source-drain doping profiles to reduce charge sharing. An interesting problem left for future study is an analysis of the tradeoff of improved subthreshold behavior at the expense of poorer drive current arising from channel doping.

Acknowledgments: The authors thank R.H. Dennard for stimulating discussions.

REFERENCES

[1] R-H. Yan, A. Ourmazd, and K.F. Lee,"Scaling the Si MOSFET: From Bulk to SOI to Bulk," *IEEE Trans. Electron Devices*, vol. 39, pp. 1704-1710, Jul. 1992.

[2] S. Veeraraghavan and J.G. Fossum,"A Physical Short-Channel Model for the Thin-Film SOI MOSFET Applicable to Device and Circuit CAD," *IEEE Trans. Electron Devices*, vol. 35, pp. 1866-1875, Dec. 1988.

[3] V.P. Trivedi and J.G. Fossum,"Scaling Fully Depleted SOI CMOS," *IEEE Trans. Electron Devices*, vol. 50, pp. 2095-2103, Oct. 2003.

[4] K. Suzuki, T. Tanaka, Y. Tosaka, H. Horie, and Y. Arimoto,"Scaling Theory for Double-Gate MOSFETs," *IEEE Trans. Electron Devices*, vol. 40, pp. 2326-2329, Dec. 1993.

[5] A. Svizhenko, M.P. Anantram, T.R. Govindam, B. Biegel, and R. Venugopal, "Two-dimensional quantum mechanical modeling of nanotransistors," *J. Appl. Phys.*, vol. 91, pp. 2343-2354, Feb. 2002.

[6] S.E. Laux, A. Kumar, and M.V. Fischetti, "Ballistic FET Modeling Using QDAME: Quantum Device Analysis by Modal Evaluation," *IEEE Trans. Nanotech.*, vol. 1, pp. 255-259, Dec. 2002.

[7] S.E. Laux, A. Kumar, and M.V. Fischetti, "Analysis of Quantum Ballistic Transport in Ultra-Small Silicon Devices Including Space-Charge and Geometric Effects," *J. Appl. Phys.*, vol. 95, pp. 5545-5582, May 2004.

[8] E. Buturla, J. Johnson, S. Furkay and P. Cottrell, "A New Three-dimensional Device Simulation Formulation," *NASECODE VI Proc.*, pp. 291-296, 1989.

[9] M. Ieong, J. Johnson, S. Furkay and P. Cottrell, "Efficient Quantum Correction Model for Multi-dimensoinal CMOS Simulations," *Proc. SISPAD 1998*, pp. 129-132, 1998.

[10] D.J. Frank, Y. Taur, and H-S. P. Wong,"Generalized Scale Length for Two-Dimensional Effects in MOSFETs," *IEEE Electron Device Lett.*, vol. 19, pp. 385-387, Oct. 1998.

Figure Captions

Figure 1: Schematic of FDSOI geometry used in this work. The BOX thickness is chosen to be 50-100 nm depending on the size of the problem. The gate metal workfunction is 200 meV above midgap. The solid and dashed lines indicate the metallurgical junctions of the source and drain (doped n-type 10^{20} cm^{-3}) for the cases of block and tapered profiles, respectively.

Figure 2: (a) Subthreshold swing (SS) as a function of body thickness for FDSOI and double-gate structures. Here $L = 15$ nm, and t_{ox}=0.5 nm. (b) Correction in SS due to quantum-mechanical effects, $\Delta \mathrm{SS}_{\mathrm{QM}}$, and two-dimensional electrostatics effects, $\Delta \mathrm{SS}_{\mathrm{el}}$, obtained by comparing results from different simulation tools in (a). Here $\Delta \mathrm{SS}_{\mathrm{QM}}$ is defined as the difference between the FIELDAY and QDAME SS values for the FDSOI structure, and $\Delta \mathrm{SS}_{\mathrm{el}}$ is defined as the difference between the FIELDAY-computed SS values for the FDSOI and double-gate structures.

Figure 3: (a) Doping transfer curve showing SS as a function of body doping for FDSOI with $L = 15$ nm, $d = 5$ nm, and t_{ox}=0.5 nm, computed semi-classically and quantum-mechanically. (b) Doping transfer curve showing SS as a function of body doping for FDSOI with $L = 30$ nm, $d = 10$ nm, and t_{ox}=1.0 nm. At high body doping, the structure becomes partially depleted, resulting in degraded SS.

Figure 4: Contours of conduction band edge (separated by 50 meV) for undoped-body FDSOI structures with (a) block and (b) tapered source-drain doping profiles. The contour lines become more vertical (less two-dimensional) when the tapered profile is used.

Figure 5: (a) Conduction band edge at 1.5 nm above the back interface, along the subthreshold leakage path, for FDSOI with tapered doping profile. As the degree of tapering is increased (r=0 to 15 nm in 5 nm increments), the potential barrier becomes both higher and thicker. Inset shows the elliptical profile used to achieve a tapered doping profile. The horizontal and vertical axes of the ellipse are r and d, respectively. (b) Subthreshold swing as a function of horizontal axis r, showing improvement with increasing tapering of source/drain doping profile. The inset shows that the improvement in subthreshold behavior comes at virtually no penalty to drive current.

Figure 6: Subthreshold swing computed using QDAME for undoped FDSOI, FDSOI with body doping 2×10^{19} cm^{-3}, and undoped double-gate structure as a function of body thickness d (double-gate structure has thickness $2d$). Dashed line shows the ratio of body thickness required to match the SS of the undoped FDSOI to that of an undoped double-gate structure.

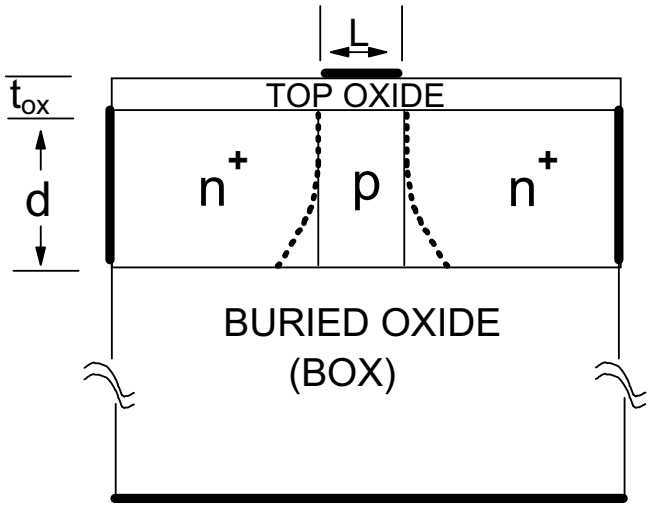

Figure 1

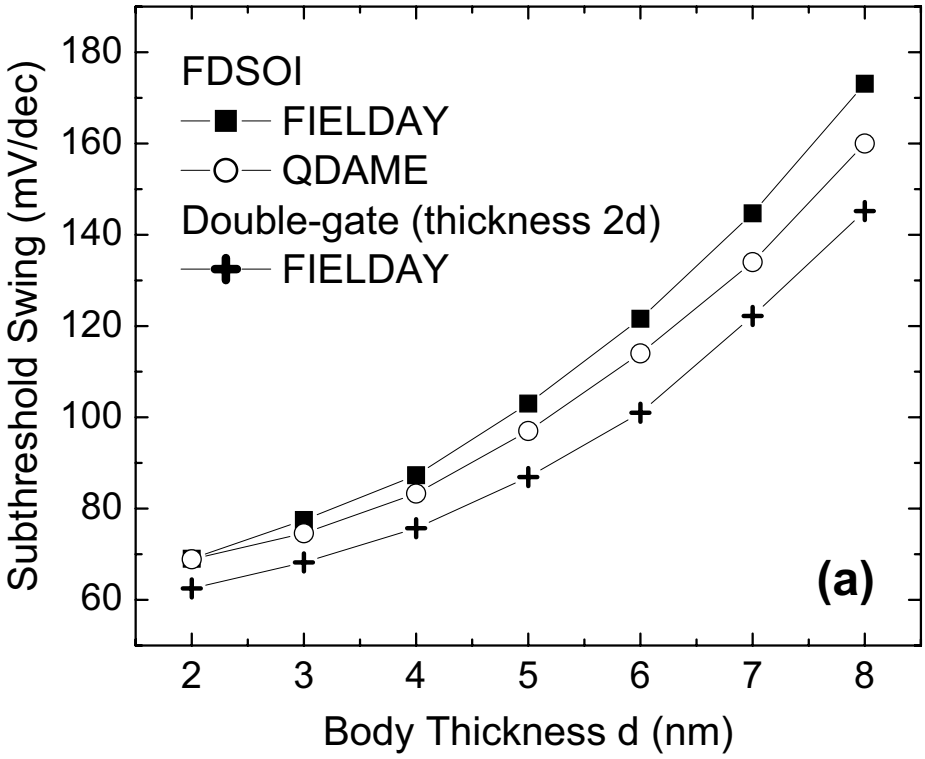
FDSOI
FIELDAY
QDAME
Double-gate (thickness 2d)
FIELDAY
(a)
Subthreshold Swing (mV/dec)
Body Thickness d (nm)
180
160
140
120
100
80
60
2
3
4
5
6
7
8

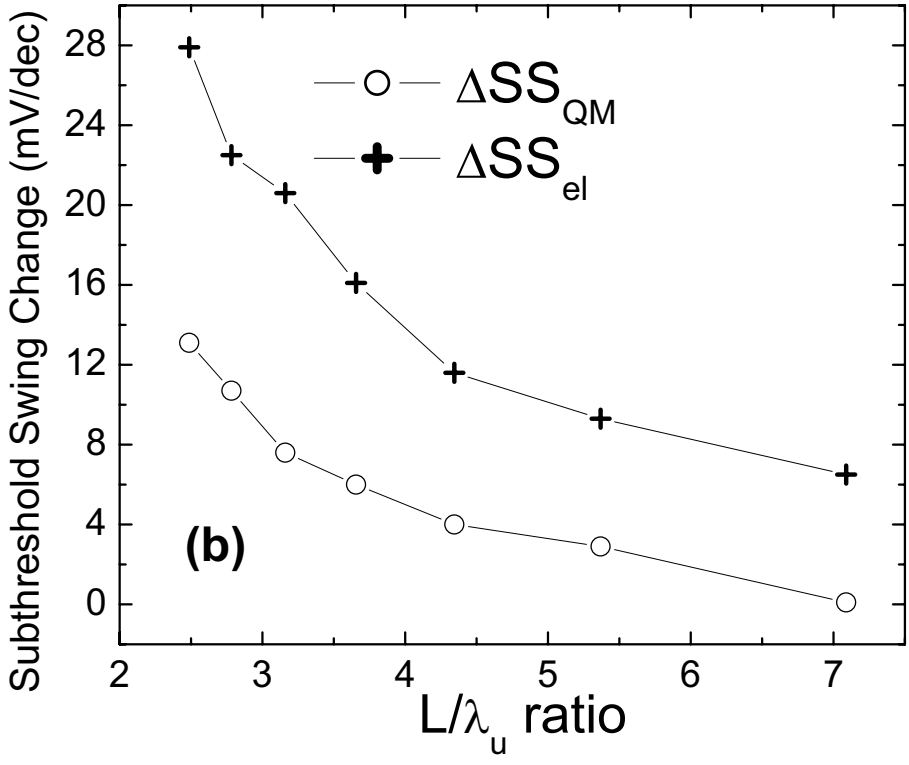
ΔSS_QM
ΔSS_el
(b)
Subthreshold Swing Change (mV/dec)
L/λ_u ratio
28
24
20
16
12
8
4
0
2
3
4
5
6
7

Figure 2

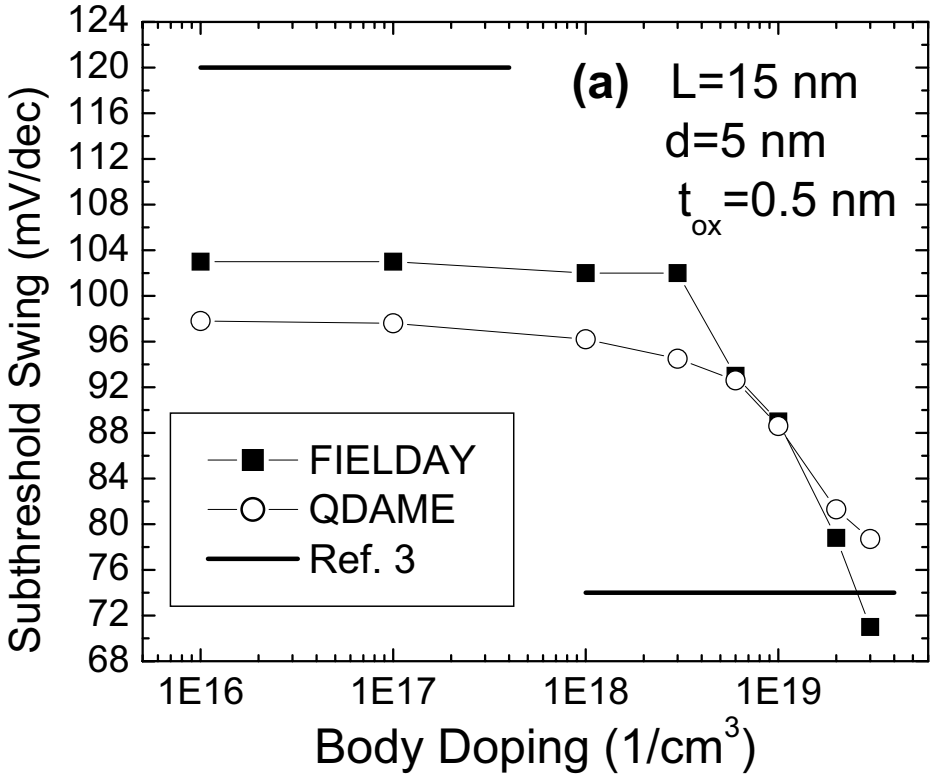
(a) L=15 nm
d=5 nm
t_ox=0.5 nm
FIELDAY
QDAME
Ref. 3
Subthreshold Swing (mV/dec)
Body Doping (1/cm^3)
124
120
116
112
108
104
100
96
92
88
84
80
76
72
68
1E16
1E17
1E18
1E19

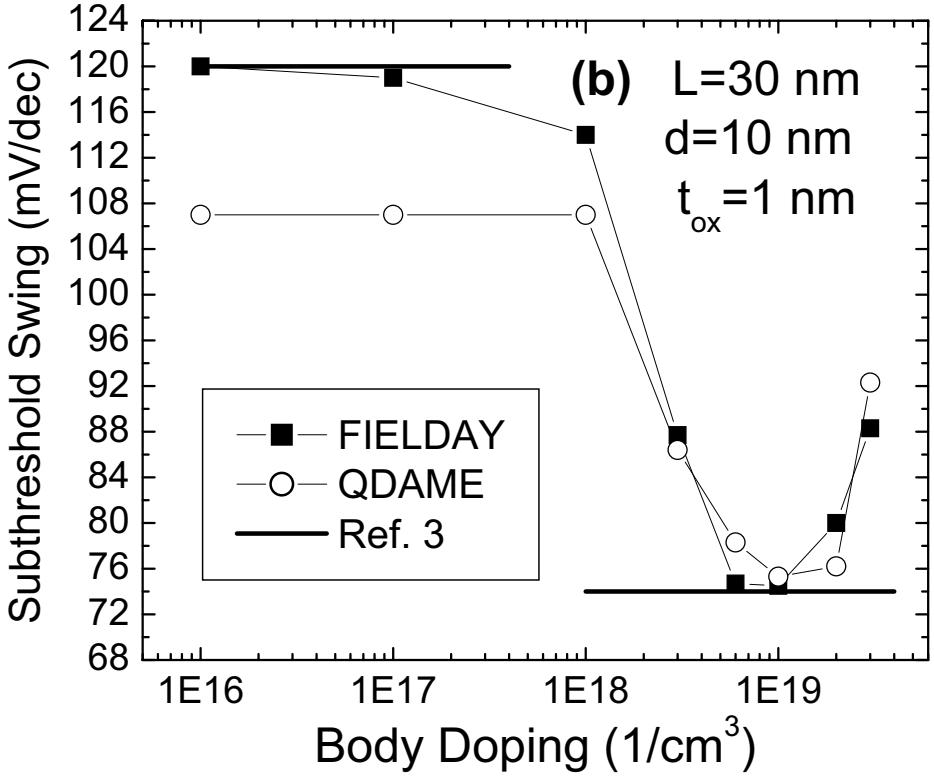
(b) L=30 nm
d=10 nm
t_ox=1 nm
FIELDAY
QDAME
Ref. 3
Subthreshold Swing (mV/dec)
Body Doping (1/cm^3)
124
120
116
112
108
104
100
96
92
88
84
80
76
72
68
1E16
1E17
1E18
1E19

Figure 3

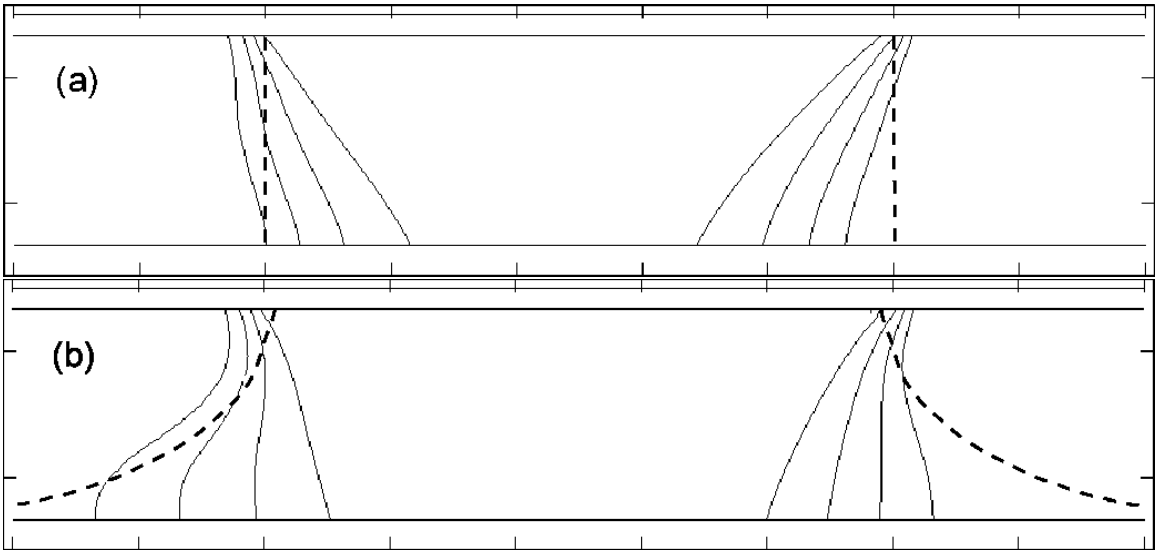

Figure 4

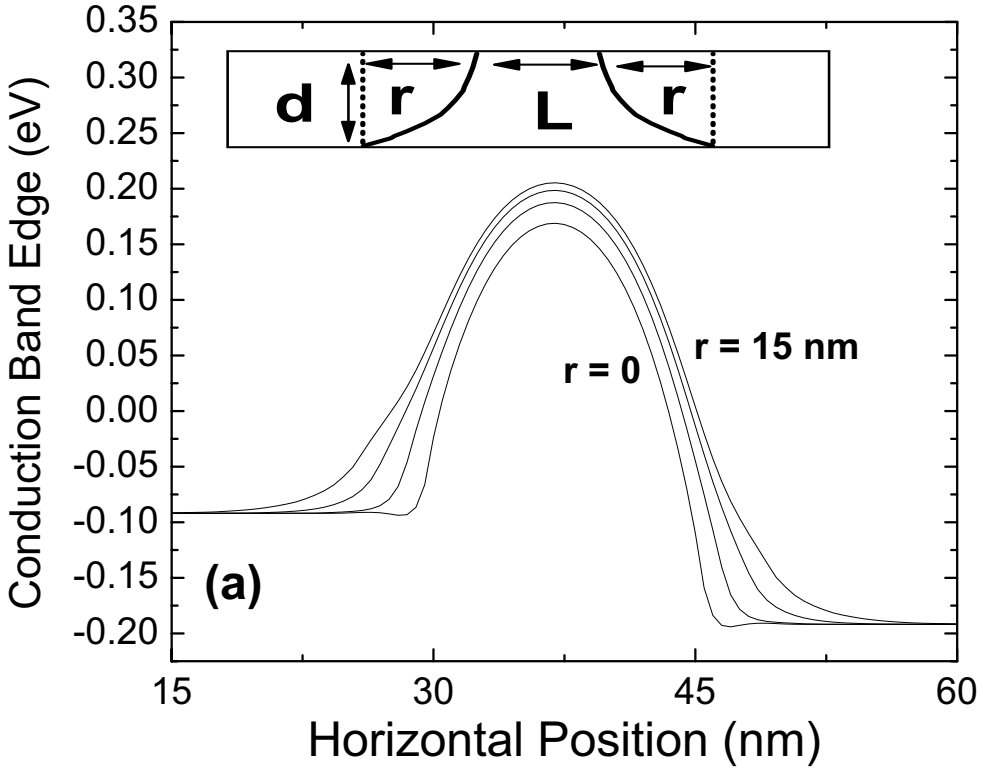
d
r
L
r
r = 15 nm
r = 0
(a)
Conduction Band Edge (eV)
Horizontal Position (nm)
0.35
0.30
0.25
0.20
0.15
0.10
0.05
0.00
-0.05
-0.10
-0.15
-0.20
15
30
45
60

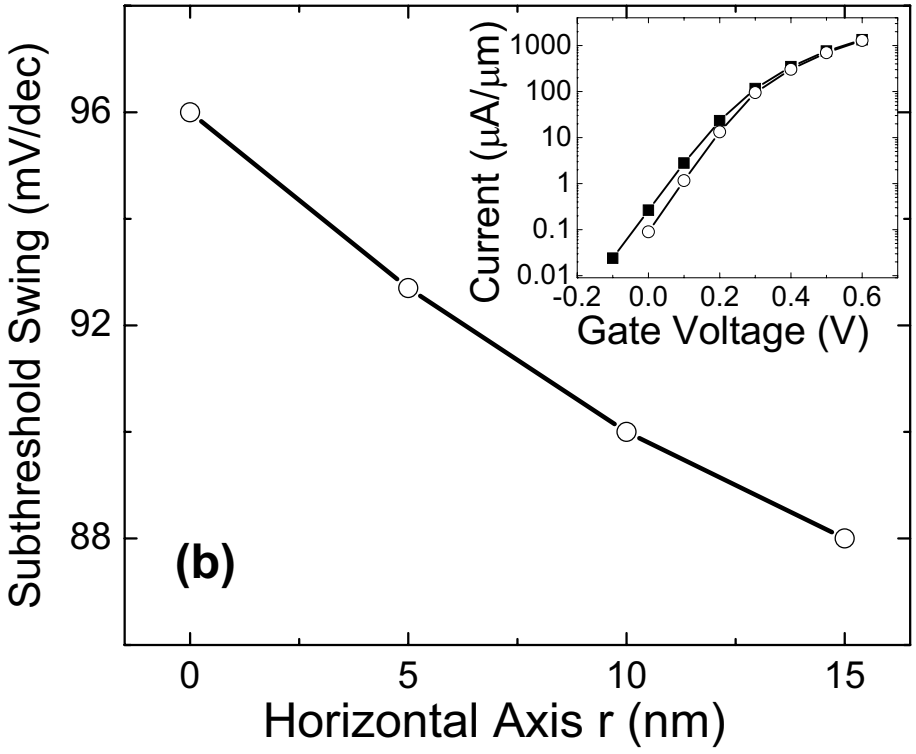
Subthreshold Swing (mV/dec)
Horizontal Axis r (nm)
(b)
96
92
88
0
5
10
15
Current (μA/μm)
Gate Voltage (V)
1000
100
10
1
0.1
0.01
-0.2
0.0
0.2
0.4
0.6

Figure 5

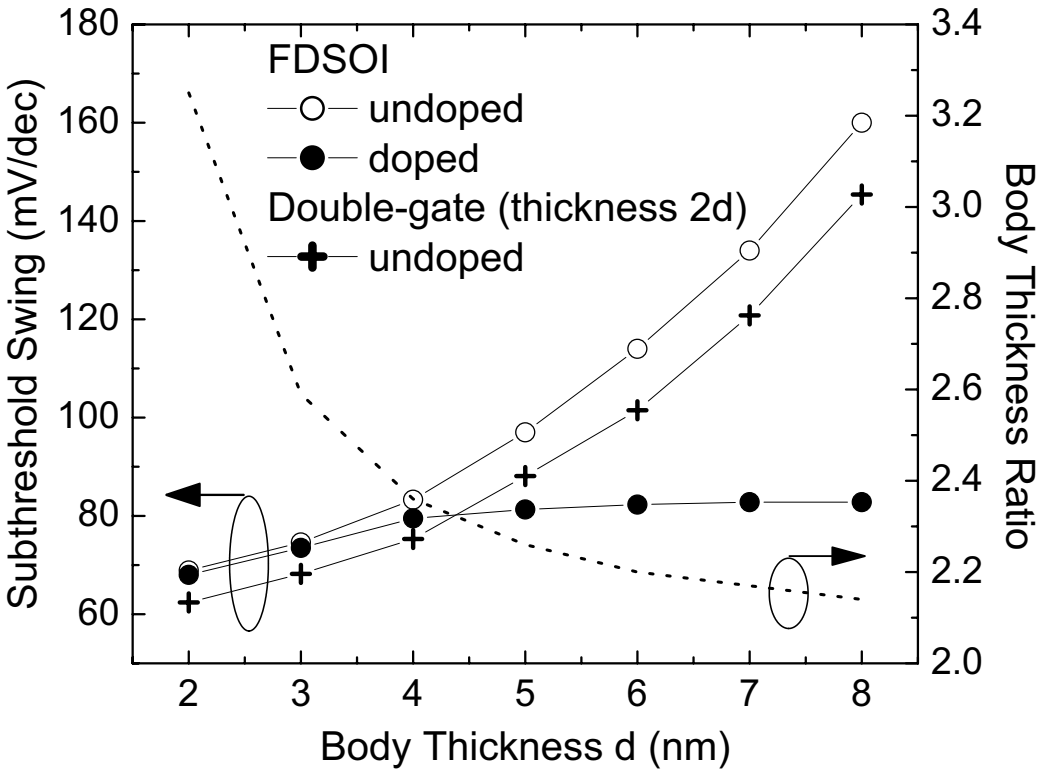
FDSOI
undoped
doped
Double-gate (thickness 2d)
undoped
Subthreshold Swing (mV/dec)
Body Thickness Ratio
Body Thickness d (nm)
180
160
140
120
100
80
60
3.4
3.2
3.0
2.8
2.6
2.4
2.2
2.0
2
3
4
5
6
7
8

Figure 6